From nodes to pathways: an edge-centric model of brain structure-function coupling via constrained Laplacians

A Preprint

Viljami Sairanen [a,b]

[a]Baby Brain Activity Center, Children's Hospital,
Helsinki University Hospital and University of Helsinki, Finland

[b]Radiology, Hämeenlinna Central Hospital, Hämeenlinna, Finland

2026-01-16

Abstract

Understanding how functional interactions emerge from the brain structure remains a central challenge in network neuroscience. Structural connectivity (SC), derived from diffusion MRI tractography, provides the anatomical scaffold, whereas functional connectivity (FC), measured with fMRI, EEG, or MEG, reflects dynamic neural interactions that often extend beyond direct anatomical links. Existing spectral graph theoretical models successfully capture indirect interactions but largely remain node-centric, leaving the contributions of individual structural pathways implicit.

This work introduces an edge-centric framework for structure-function coupling that reformulates the graph Laplacian as a constrained flow problem grounded in spectral graph theory and realized numerically

through Modified Nodal Analysis (MNA). Functional relationships are modeled as nodal constraints (voltage sources), structural connections as conductances, and the resulting nodal potentials induce edge-wise flows (currents) that explicitly quantify how functional signals are distributed in anatomical network. This formulation preserves the theoretical foundations of Laplacian eigenmodes while extending them to compute interpretable, pathway-specific measures of functional signal flow.

As a proof-of-concept, the framework is demonstrated in three settings: (i) a single-subject Default Mode Network example illustrating tractography filtering and streamline-wise functional currents, (ii) a ground-truth diffusion phantom showing accurate recovery of both direct and indirect pathways, and (iii) a group-level analysis of 207 Human Connectome Project subjects yielding a sparse, current-based connectome complementary to conventional SC and FC matrices. By bridging spectral graph theory and circuit analysis, this approach provides a mathematically consistent and physically interpretable method for mapping functional interactions onto structural brain networks, with practical applications in tractography filtering, network analysis, and multimodal connectomics.

Keywords Brain Connectivity · Structure–Function Coupling · Graph Laplacian · Modified Nodal Analysis (MNA) · Tractography Filtering

1 Introduction

Understanding how structural connectivity (SC) relates to functional connectivity (FC) is a central challenge in network neuroscience (Greaves et al., 2025). SC provides the anatomical scaffold of axonal pathways, often measured using diffusion-weighted MRI tractography, whereas FC is typically characterized as statistical dependencies in neural activity measured via fMRI, EEG, or MEG. Although SC and FC exhibit macroscale correlations (Honey et al., 2009), many functional relationships occur without a

direct structural link, reflecting polysynaptic and network-mediated interactions and motivating computational models that formalize this coupling.

A prominent class of approaches to couple SC and FC relies on spectral graph theory (Chung, 1997), which uses the graph Laplacian of the SC network and its eigendecomposition to model functional relations. For example, network diffusion models (Abdelnour et al., 2014) predict FC by simulating heat-like diffusion on the SC graph, while spectral models (Abdelnour et al., 2018; Atasoy et al., 2016; Deslauriers-Gauthier et al., 2020) express FC patterns as combinations of connectome harmonics. These harmonics correspond to Laplacian eigenmodes that capture indirect pathways and polysynaptic interactions. These approaches exploit the eigendecomposition of the Laplacian to reveal fundamental modes of network communication, providing a principled link between structure and function grounded in graph signal processing (Shuman et al., 2013).

Despite their success, existing Laplacian related network models primarily yield node level descriptions of structure-function coupling, in which functional interactions are summarized between pairs of regions. While such models implicitly account for multi-edge pathways, they do not explicitly identify which structural connections or tractography streamlines support a given functional relationship. As a result, the contributions of individual edges or specific structural pathways to functional communication remain latent and difficult to interpret. Moving beyond node-level representations toward an edge-centric perspective offers a route-based view of structure-function coupling, enabling the tracing of information flow through concrete anatomical pathways.

A wide range of alternative computational approaches have also been proposed to link brain structure and function. Some model biophysical dynamics (Breakspear et al., 2010; Deco, 2015; Liu et al., 2022), others perform statistical correlations between the connectomes (Huang and Ding, 2016; Suárez et al., 2020), or apply machine learning methods such as Graphical Neural Networks (GNNs) (Chen et al., 2024; Hong et al., 2023; Neudorf et al., 2022; Yang et al., 2022; Zalesky et al., 2024). While these methods differ in formulation and expressive power, they similarly focus on predicting

node-level functional connectivity patterns, offering limited insight into the specific structural pathways that mediate functional interactions.

This study builds on the graph Laplacian-based approaches and introduce a framework that moves beyond node-level representations to compute how functional information traverses through the edges of the structural connectome graph. By formulating structure-function coupling as a constrained Laplacian problem, functional relationships are mapped onto structural pathways, yielding interpretable measures of how functional correlations traverse the structural network. The proposed edge-centric perspective adds a new dimension to graph-based network analyses by providing connection and tractography streamline specific insights that may help in uncovering mechanisms underlying brain disorders and conditions. Beyond its theoretical contribution, the framework enables practical applications such as identifying structural connections that preferentially support functional coupling and informing tractography filtering using functional data. To facilitate adoption, an open-source Python implementation for applying this framework to existing SC and FC datasets is freely available in Github[1].

2 Theory

Spectral graph theory provides a principled framework for modeling signal interactions within networks, with the graph Laplacian encoding conservation of flow across nodes (Chung, 1997; Shuman et al., 2013). In network neuroscience, Laplacian eigendecomposition has been used to characterize structure-function relationships at the graph node level (Honey et al., 2009).

This section builds on this theory and describes an idea of how the Laplacian eigendecomposition could be extended to define nodal potentials originating from the functional brain signals whose graph gradients result in edge-level patterns describing how functional information is distributed within the structural network.

[1]https://github.com/vilsaira/FSC

2.1 Graph Laplacian equality between node and edge spaces

The structural connectome can be represented as an undirected weighted graph $G = (V, E, W)$ where V are brain region nodes, E are edges i.e. white-matter connections between the regions, and W is the weighted adjacency matrix that encode nodewise structural connection strength such as number of streamlines, for example, and is given by:

$$W_{ij} = \begin{cases} w_{ij} & (i,j) \in E \\ 0 & \text{otherwise} \end{cases} \tag{1}$$

The degree matrix of graph G is given by $D = \operatorname{diag}\left(\sum_j w_{ij}\right)$.

In the case of weighted graph, the graph Laplacian operator acts on nodewise signals as $(\mathcal{L}f)(i) = \sum_j w_{ij}\,(f(i) - f(j))$ and leads to two equivalent matrix representations of the graph Laplacian. The first representation is in node space:

$$\mathcal{L} = D - W \tag{2}$$

and the second representation is in edge space:

$$\mathcal{L} = BCB^{\top}, \tag{3}$$

where B is oriented incidence matrix and $C = \operatorname{diag}(e_w), \quad e \in E$ is edge weight matrix (Chung, 1997; Shuman et al., 2013). Structural edge weights C quantify how easily interactions can traverse between regions. By combining equations 2 and 3, the mapping between node and edge representations of graph Laplacian is given by

$$D - W = BCB^{\top}. \tag{4}$$

2.2 From Laplacian eigenmodes to nodal potentials

The equivalence in eq. 4 shows that the graph Laplacian leads to both a node-centric and an edge-centric interpretations. In the node-space formulation, the Laplacian characterizes how signals defined on regions differ from their neighbors, whereas in the edge-space formulation it encodes how such differences are distributed along individual structural connections.

To relate graph Laplacian operator to brain functions, consider a scalar-valued nodal field $\phi \in \mathbb{R}^{|V|}$. This can be interpreted as a nodal potential originating from the functional information, and it can be solved from the following Laplacian system

$$\mathcal{L}\phi = \mathbf{s}, \tag{5}$$

where $\mathbf{s} \in \mathbb{R}^{|V|}$ represents nodal source terms that encode functional constraints or external inputs imposed on the structural network. With the properties of graph Laplacian, ϕ can be solved using the Moore-Penrose pseudoinverse

$$\phi = \mathcal{L}^{\dagger}\mathbf{s}. \tag{6}$$

The eigendecomposition of the Laplacian $\mathcal{L} = U\Lambda U^{\top}$ where $U = [\mathbf{u}_1, ..., \mathbf{u}_{|V|}]$ is an orthonormal matrix whose columns $\mathbf{u}_k \in \mathbb{R}^{|V|}$ are the eigenvectors of the graph Laplacian and $\Lambda = \mathrm{diag}(\lambda_1, ..., \lambda_{|V|})$ is the diagonal matrix of Laplacian eigenvalues leads to expression

$$\phi = \sum_{k=2}^{|V|} \frac{1}{\lambda_k} \left(\mathbf{u}_k^{\top}\mathbf{s}\right) \mathbf{u}_k, \tag{7}$$

demonstrating that nodal potentials are linear combinations of Laplacian eigenmodes, weighted by the inverse of their eigenvalues. Indexing starts from $k = 2$ because the first eigenvalue of the graph Laplacian is zero corresponding to the constant mode which is excluded by the definition of the Moore-Penrose pseudoinverse. This

spectral representation is related to prior work showing that low-frequency Laplacian eigenmodes dominate macroscale functional organization and capture indirect, polysynaptic interactions in the brain (Abdelnour et al., 2018, 2014; Atasoy et al., 2016; Deslauriers-Gauthier et al., 2020).

2.3 Mapping nodal information to edges with graph gradients

If the nodal potentials ϕ describe the spatial distribution of functional signals, the graph gradient operator ∇_G of it represents how the functional interactions are mediated along structural pathways:

$$\nabla_G \phi := B^\top \phi, \tag{8}$$

that assigns the difference in potential between incident nodes of each edge. Weighting this gradient by the edge-weight matrix C yields a definition for edge-wise flow $\mathbf{f}$:

$$\mathbf{f} := CB^\top \phi, \tag{9}$$

whose elements $\mathbf{f}_e = e_w(e)(\phi_i - \phi_j)$ quantifies how strongly a functional potential difference is supported by the corresponding structural connection. In this sense, edge weights act as pathway-specific gains that modulate the transmission of functional information.

Substituting the eigenmode expansion in eq. 7 into eq. 9 gives

$$\mathbf{f} = \sum_{k=2}^{|V|} \frac{1}{\lambda_k} \left(\mathbf{u}_k^\top \mathbf{s}\right) CB^\top \mathbf{u}_k, \tag{10}$$

showing that edge flows correspond to weighted spatial derivatives of Laplacian eigenmodes, providing an explicit pathway-level realization of connectome harmonics. Therefore eq. 10 maps nodal functional information $\mathbf{s}$ onto structural graph G, yielding an edge-level representation consistent with the brain anatomy.

While existing structure–function coupling models implicitly account for multi-edge pathways, they typically summarize interactions at the node or region level, leaving the contributions of individual structural connections hidden (Greaves et al., 2025; Sporns, 2013; Suárez et al., 2020). To my knowledge, this edge-resolved spectral representation has not been previously explored in network neuroscience and therefore could provide new insights to brain network analyses.

3 Methods

This section is separated into four parts: The numerical framework used in the proposed function-structure coupling 3.1, single subject example of tractogram filtering in Default Mode Network (Raichle et al., 2001) analysis 3.2, a ground-truth phantom simulation 3.3, group-level analysis of 207 subjects of the Human Connectome Project (Van Essen et al., 2012) 3.4.

3.1 Constrained Laplacian as Modified Nodal Analysis problem

Section 2 formulated structure–function coupling as a constrained Laplacian problem $\mathcal{L}\phi = \mathbf{s}$ (eq. 5), in which functional relationships impose nodal constraints on a structural graph and induce edge-level flows. This section builds on that formulation and describes how this system is solved numerically using Modified Nodal Analysis (MNA) (Ho et al., 1975; Wedepohl and Jackson, 2002), without altering the underlying theoretical formulation.

Structural connectivity is represented by the weighted graph Laplacian $\mathcal{L}$, and the source vector $\mathbf{s}$ encodes functional constraints. Rather than solving the constrained system via explicit pseudoinversion or eigendecomposition, MNA is used as it results in an equivalent but computationally efficient sparse linear system and physically interpretable results.

3.1.1 Modified Nodal Analysis (MNA) formulation

Functional constraints are incorporated with an incidence matrix $B \in \mathbb{R}^{n\times m}$, with corresponding constraint values $\mathbf{s} \in \mathbb{R}^m$. This gives the following MNA system

$$\begin{bmatrix} \mathcal{L} & B \\ B^\top & 0 \end{bmatrix} \begin{bmatrix} \phi \\ \mathbf{i}_s \end{bmatrix} = \begin{bmatrix} 0 \\ \mathbf{s} \end{bmatrix} \tag{11}$$

where $\phi \in \mathbb{R}^n$ are nodal potentials (same as in Section 2), $\mathbf{i}_v \in \mathbb{R}^m$ are auxiliary variables that enforce the constraints (Ho et al., 1975; Wedepohl and Jackson, 2002). To avoid singularity, one node is grounded (e.g., $\phi_1 = 0$) This system is symmetric, semi-definite, and sparse, ensuring computational efficiency even for large connectomes. This formulation provides a numerical realization of the constrained Laplacian system of eq. 5, without altering its theoretical interpretation.

3.1.2 Graph edge flows

Once nodal potentials ϕ are solved using MNA, flows along structural edges can be computed using eq. 9 or in element-wise form:

$$I_{ij} = w_{ij}(\phi_i - \phi_j). \tag{12}$$

These values define an edge-centric connectivity matrix I that quantifies how functional information is distributed through individual structural connections. In the absence of functional constraints, the formulation reduces to a homogeneous Laplacian system equivalent to standard diffusion models of spectral graph theory.

3.2 Default Mode Network example

To demonstrate the proposed function-structure coupling method, one subject was selected from the Human Connectome Project (HCP) because this dataset provides both preprocessed resting-state fMRI (including ICA-derived components) and diffusion-weighted MRI tractography. This combination enables direct comparison of functional and structural connectivity within the same individual.

The Default Mode Network (DMN) was chosen as a test case due to its well-characterized role in intrinsic brain activity and strong structure–function associations. A DMN atlas (Smith and Nichols, 2009) was used to identify the ICA component

with the highest spatial correlation to the DMN template. The resulting mask was segmented into six regions of interest (ROIs): medial prefrontal cortex (mPFC), posterior cingulate cortex (PCC), left and right inferior parietal lobules (IPL), and left and right temporal lobes (TL).

Functional connectivity between these ROIs was computed as Pearson's correlation coefficient of the average fMRI time series within each region. This produced a 6x6 functional connectivity matrix representing pairwise correlations.

Whole-brain tractography was performed using MRtrix (Tournier et al., 2019) with multi-shell, multi-tissue constrained spherical deconvolution (Dhollander et al., 2016; Smith et al., 2012). Parameters included one million streamlines, minimum and maximum lengths of 5 mm and 250 mm, and a normalized white matter FOD cutoff of 0.05. The structural connectivity matrix was constructed by counting streamlines connecting each pair of DMN ROIs.

The functional and structural matrices were coupled using the MNA-based approach described in Section 3.1. Nodal voltages were solved from the simplified MNA system (eq. 11), and currents along structural edges were computed using eq. 12. These currents represent the estimation how the of functional information disperses through anatomical pathways.

The resulting current matrix highlights which structural connections carry the most functional signal. For visualization, tractograms were filtered to retain streamlines with non-zero currents, and streamline-wise currents are shown with color scaling. This provides an intuitive representation of how functional correlations traverse the structural network.

This single-subject example illustrates the feasibility of the proposed method and sets the stage for group-level analyses described in Section 2.4.

3.3 Ground-truth simulation

To validate the proposed method under controlled conditions, we used the FiberCup phantom (Fillard et al., 2011; Poupon et al., 2010, 2008), which provides a simplified

yet anatomically plausible structure with known ground truth. This phantom is ideal for testing both direct and indirect functional relationships.

The phantom was divided into five functional subnetworks (figure 4 A). Four subnetworks were designed as direct connections between nodes, while the fifth included an indirect pathway through an intermediate node. A U-shaped structure served as a control to verify that unrelated regions do not influence other subnetworks. Functional correlation strength was set uniformly to 1 for all subnetworks.

Diffusion-weighted data were processed using MRtrix (Tournier et al., 2019) with constrained spherical deconvolution to generate one million streamlines, ensuring coverage of all phantom pathways.

The proposed MNA-based coupling was applied to compute nodal voltages and edge currents. These currents were then used to filter the tractogram, removing streamlines that did not contribute to functional information flow.

Performance was assessed in two ways: (i) visual inspection of global filtering of the entire tractogram before and after filtering (figure 4 B-C), and (ii) subnetwork correctness—verification that each functional network retained only its relevant structural connections (figure 5). The method successfully removed unnecessary structural segments and correctly identified indirect pathways without false positives.

This simulation demonstrates that the proposed approach can accurately map functional relationships onto structural pathways, even in cases involving indirect connections.

3.4 Group study example

To assess the generalizability of the proposed method, we applied it to a cohort of 207 unrelated healthy adults from the HCP (Larivière et al., 2020; Van Essen et al., 2012). This group-level analysis demonstrates how the new dimension from the function-structure coupling produces a complementary connectivity matrix at the population scale.

Functional and structural connectivity matrices were obtained using the ENIGMA Toolbox (Larivière et al., 2021). The Desikan–Killiany atlas was selected for parcellation, resulting in 68 cortical regions per subject. Functional connectivity was computed from resting-state fMRI as Fisher z-transformed correlations, while structural connectivity was derived from diffusion MRI tractography.

Subject-level matrices were averaged to create group-level structural and functional connectomes. These were then coupled using the MNA-based approach described in Section 3.1 to compute the new connectome from eq. 12.

4 Results

A single subject (100307) and a dataset of an unrelated cohort of 207 healthy adult subjects from the Human Connectome Project (Larivière et al., 2021; Van Essen et al., 2012) were used in this study. The human examples provided real world demonstrations of the applicability of the proposed method. Complementary to human data, a simulation based on the FiberCup phantom (Fillard et al., 2011; Poupon et al., 2010, 2008) was used to provide a more intuitive demonstration of the method with known ground-truth specifications.

4.1 Default Mode Network example

To illustrate the practical application of the proposed function-structure coupling framework, the Default Mode Network (DMN) from a HCP subject was analyzed. This dataset was selected because it provides both diffusion MRI tractography and preprocessed resting-state fMRI, enabling direct comparison of structural and functional connectivity within the same individual.

The DMN was chosen as a test case due to its well-established role in intrinsic brain activity and its strong structure-function associations. An ICA volume with the highest spatial correlation to the DMN atlas (Smith and Nichols, 2009) was identified, spatially smoothed, and thresholded to produce subject-specific DMN nodes, shown in figure 1. The six regions identified correspond approximately to the medial prefrontal

cortex (mPFC), posterior cingulate cortex (PCC), bilateral inferior parietal lobules (IPL), and bilateral temporal lobes (TL). This experiment is not intended to redefine the DMN but to demonstrate how the proposed coupling algorithm can be applied to any network configuration.

The subject's DMN mask was used to extract all diffusion MRI tractography streamlines connected to the DMN, as shown in figure 3A. These streamlines were then filtered using the function-structure coupling approach, removing those with zero or near-zero current, as illustrated in figure 2B. Streamline-wise currents were applied as a colormap in the latter image to highlight which structural pathways carry the most functional information. Finally, Figure 3 illustrates how streamline-wise currents can be visualized alongside nodal potentials, yielding an interpretable representation of how functional coupling is distributed across anatomical connections.

4.2 Ground-truth simulation

To evaluate the proposed method under controlled conditions, the FiberCup phantom (Fillard et al., 2011; Poupon et al., 2010, 2008) was used as it provides a simplified yet anatomically plausible structure with known ground truth. This setup allows testing of both direct and indirect functional relationships.

The phantom was divided into five functional subnetworks, as shown in figure 4 A. Four subnetworks involved direct structural connections, while the fifth required an indirect pathway through an intermediate node. A U-shaped structure served as a control to confirm that unrelated regions do not influence other subnetworks.

After applying the proposed function-structure coupling, the tractogram was filtered to retain only streamlines supporting functional information flow. Figure 4 B-C illustrates this effect: unnecessary structural segments were removed, leaving only relevant pathways. Subnetwork-level results are shown in figure 5, where all subnetworks were correctly identified without false positives. The indirect pathway was also reconstructed accurately, with lower currents reflecting its higher resistance.

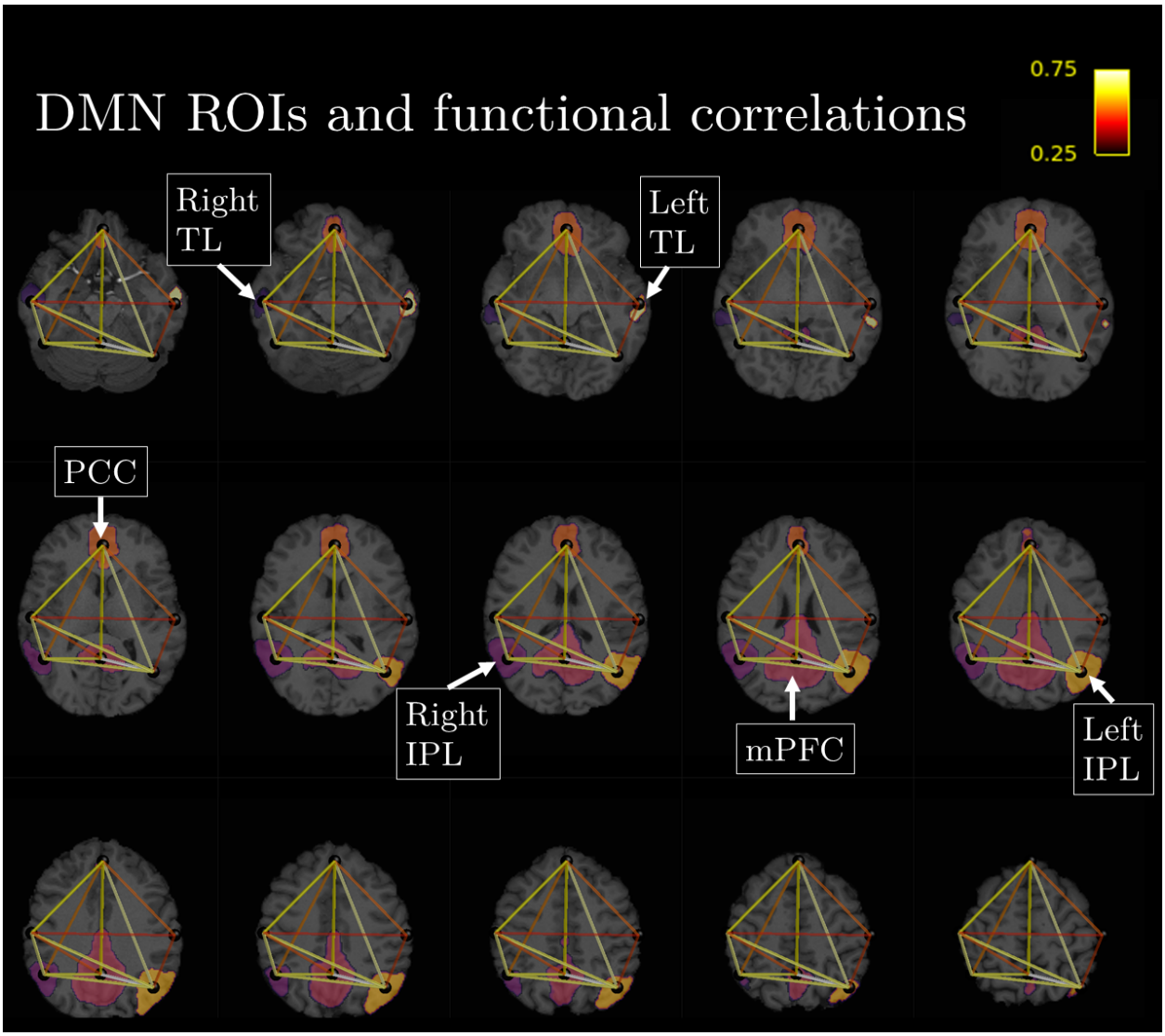

Figure 1: Visualization of the subject's Default Mode Network (DMN). Six regions of interest are shown in distinct colors: medial prefrontal cortex (mPFC), posterior cingulate cortex (PCC), left and right inferior parietal lobules (IPL), and left and right temporal lobes (TL). The accompanying graph depicts functional connectivity between these regions, with edge color indicating the strength of functional correlations.

4.3 Group studies

To assess the generalizability of the proposed method, ít was applied to a cohort of 207 unrelated healthy adults from the Human Connectome Project (Van Essen et al., 2012). Group-level structural and functional connectivity matrices were computed using the Desikan–Killiany atlas and averaged across subjects (Larivière et al., 2021). These

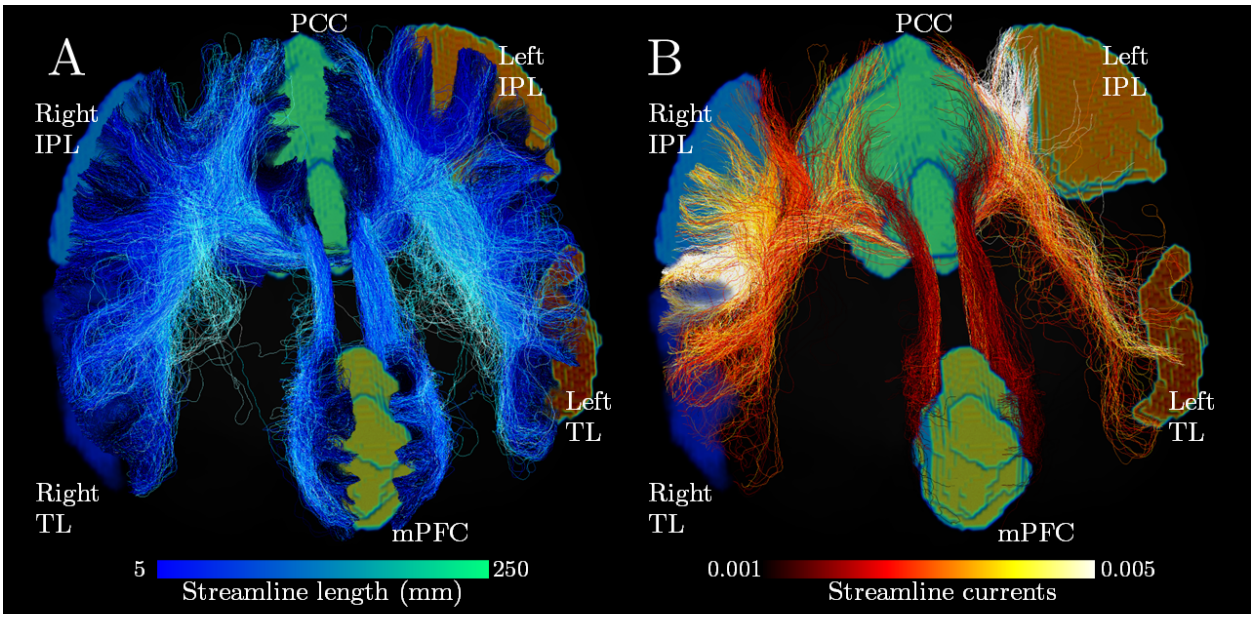

Figure 2: Tractography filtering using constrained Laplacian structure–function coupling in a single subject Default Mode Network (DMN). (A) Original tractogram connecting the six DMN regions, with streamline color indicating length. (B) Tractogram after filtering based on the current-based coupling, where streamlines carrying negligible current have been removed. Remaining streamlines are color-coded by streamline-wise current magnitude. The reduction in streamlines reflects selective retention of structural pathways that efficiently support the observed functional relationships, rather than uniform use of all anatomically reconstructed connections. This sparsification emphasizes pathways most consistent with the functional coupling pattern while suppressing weak or redundant trajectories inherent to tractography.

matrices were then coupled using the proposed framework to derive a current-based connectome.

Figure 6 compares the functional (red) and structural (blue) connectivity matrices with the resulting current-based connectome (green). Notably, the current-based connectome appears sparser than either of the original matrices, suggesting that functional signals often converge along shared structural pathways rather than being distributed across all anatomical connections. This group-level analysis demonstrates that the proposed approach provides a complementary connectivity representation at the population scale, offering insights into how functional information traverses through structural networks.

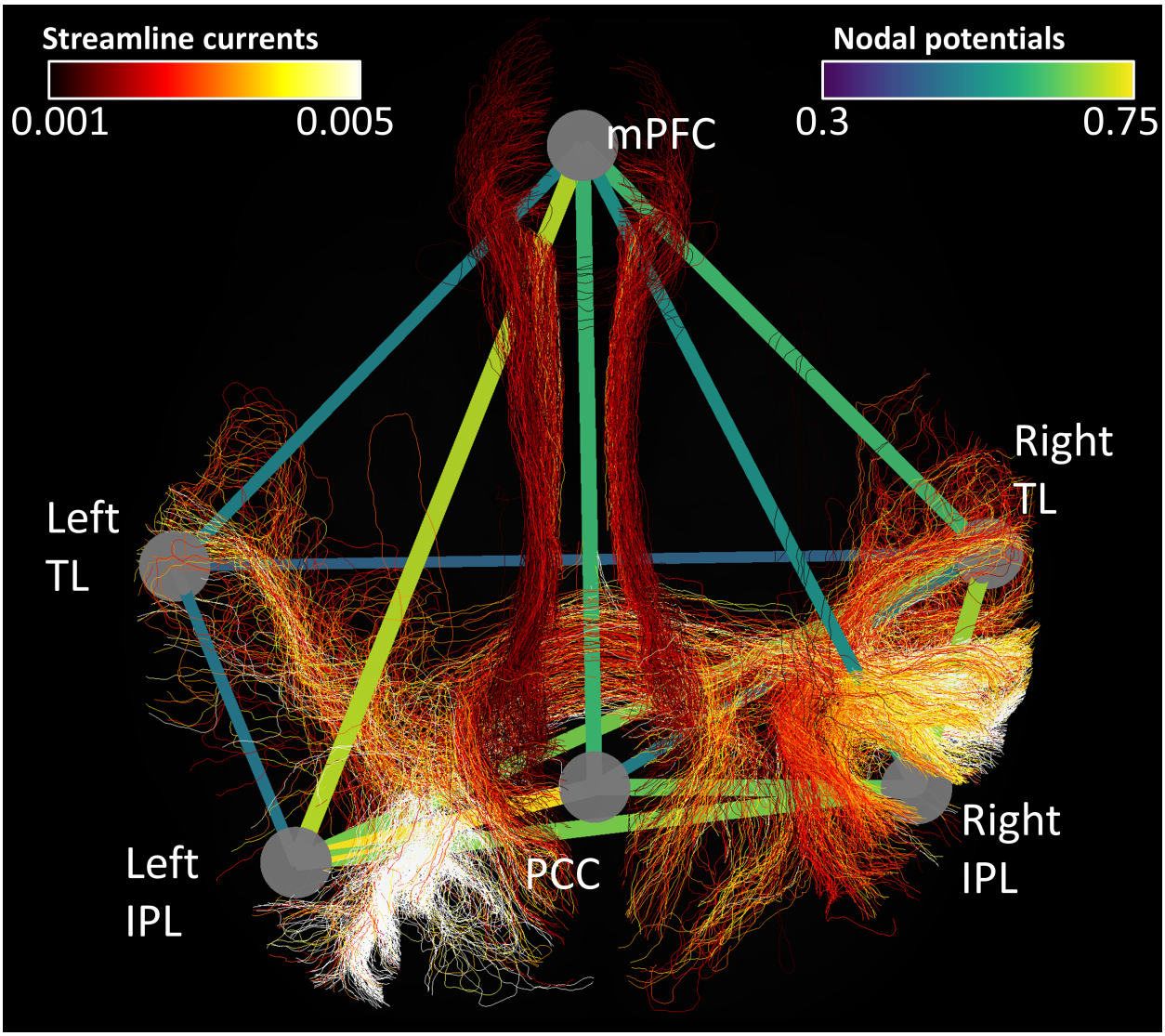

Figure 3: Visualization of nodal voltages and streamline-wise currents within the subject's DMN. The graph depicts nodal voltages, with edges representing voltage drops between regions. Overlaid tractography streamlines are color-coded by corresponding functional current values, highlighting structural pathways that carry the most functional information. This combined representation provides an interpretable view of how functional signals traverse through anatomical connections.

5 Discussion

This study investigated whether Modified Nodal Analysis (MNA), a method traditionally used in electrical circuit theory (Ho et al., 1975; Wedepohl and Jackson, 2002), can be adapted to study macroscale brain connectivity. Crucially, the proposed framework is firmly grounded in spectral graph theory (Chung, 1997; Shuman et al.,

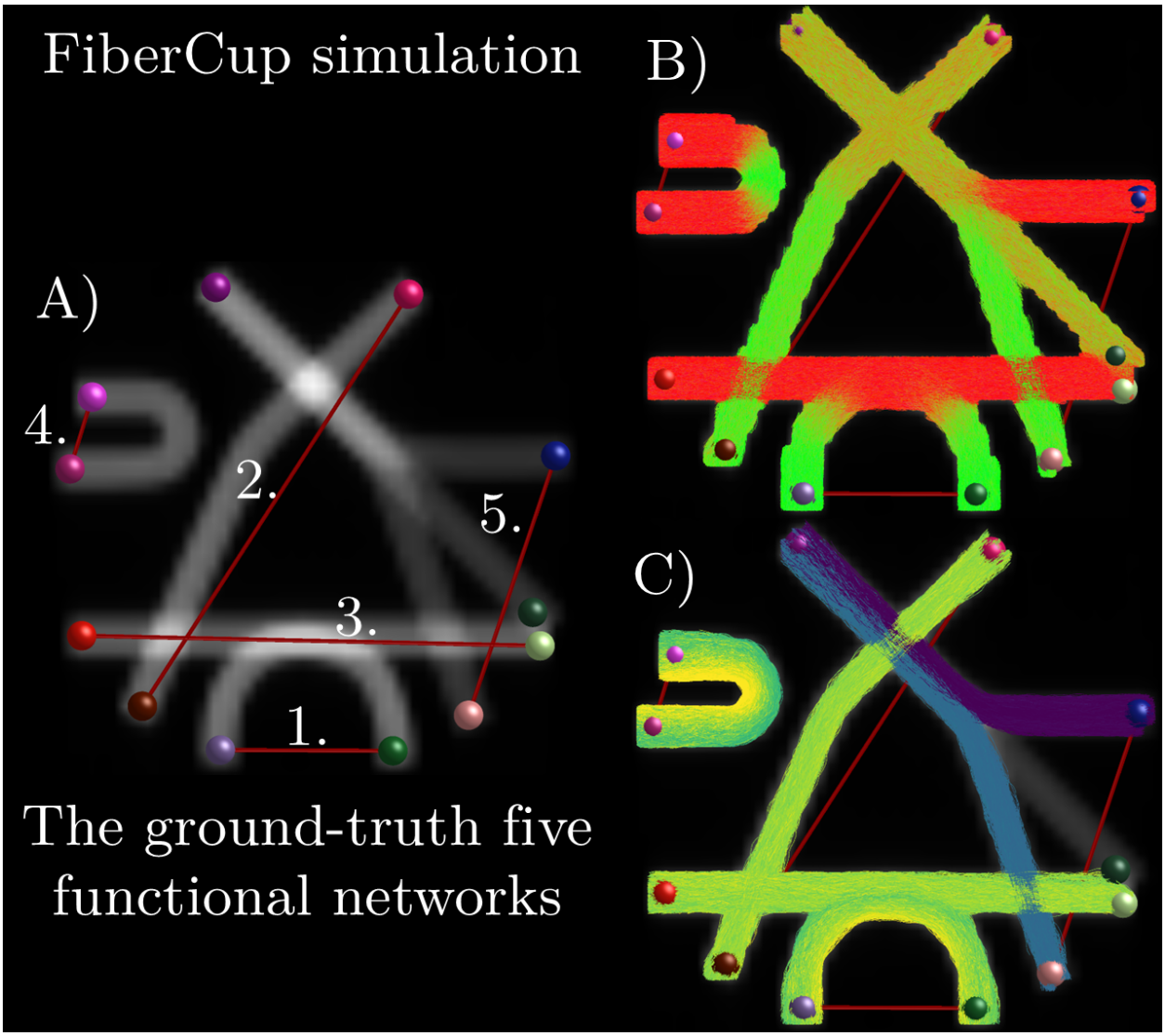

Figure 4: Ground-truth phantom simulation using the FiberCup dataset. Panel A illustrates the phantom divided into five simulated functional subnetworks, with the fifth network involving an indirect connection. Panel B shows the complete tractogram of the phantom, depicting all structural pathways. Panel C demonstrates the filtered tractogram after applying the proposed function–structure coupling, where unnecessary structural segments have been removed. This result confirms the algorithm's ability to identify optimal pathways for functional information flow.

2013), as it reformulates the Laplacian constraint into an MNA system. This preserves the core principle of signal conservation across nodes while extending it to compute edge-level currents, offering a physically interpretable representation of functional signal traverses through structural pathways. However, it is important to acknowledge

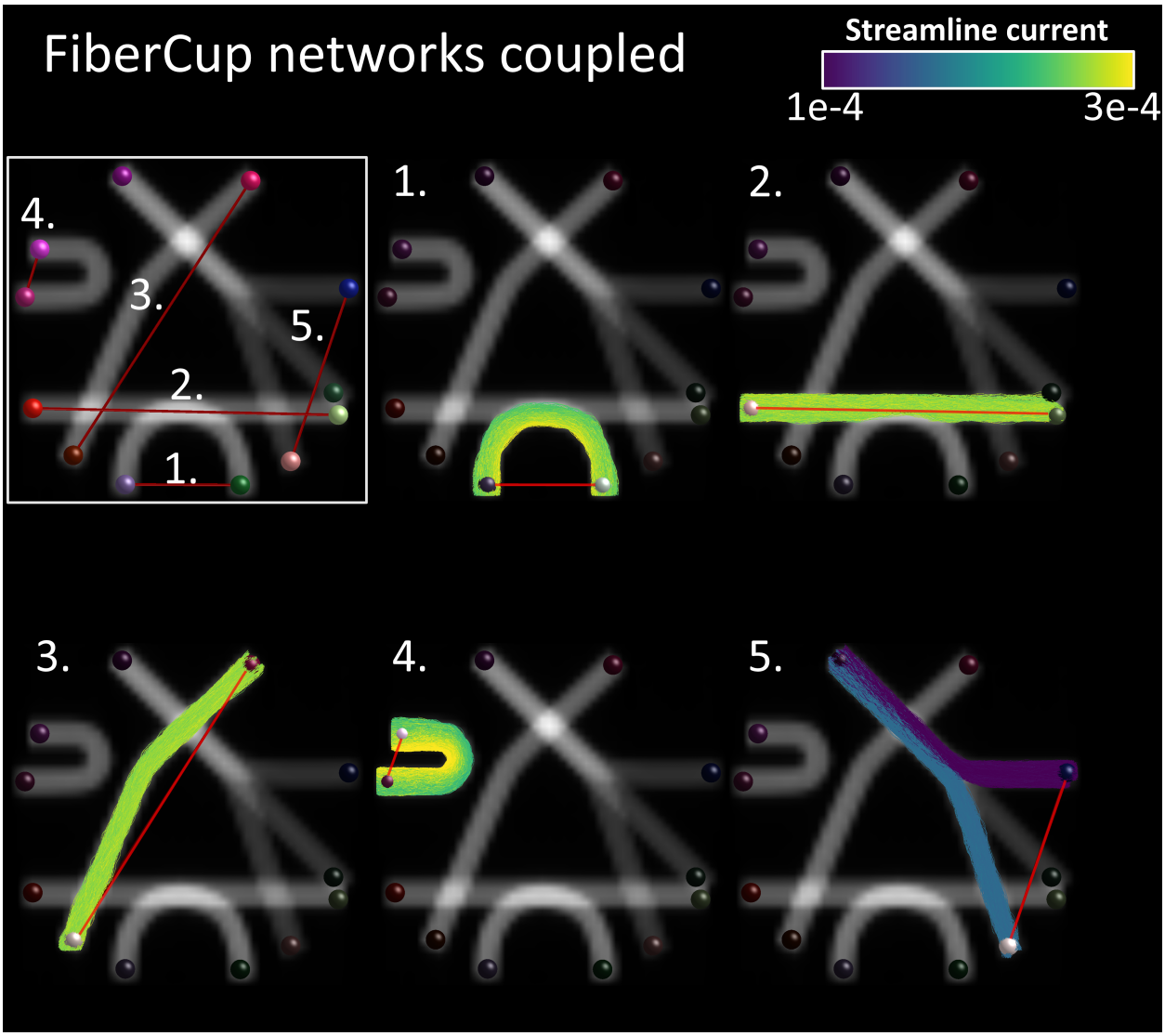

Figure 5: Subnetwork-level analysis of the FiberCup phantom simulation. Each panel shows the retained structural pathways for one of the five functional subnetworks after filtering. All subnetworks are correctly identified without false-positive connections. The fifth subnetwork, which involves an indirect pathway, is also accurately reconstructed. Color coding reflects streamline-wise current, which is lower for the indirect pathway due to its higher resistance and longer travel distance.

that the method inherits limitations from the underlying structural and functional connectivity estimates, including tractography biases and fMRI noise.

Spectral graph theory has provided a principled foundation for modeling structure-function coupling, with approaches such as connectome harmonics and diffusion models leveraging Laplacian eigenmodes to capture indirect pathways and polysynaptic interactions (Abdelnour et al., 2018, 2014; Atasoy et al., 2016; Deslauriers-Gauthier

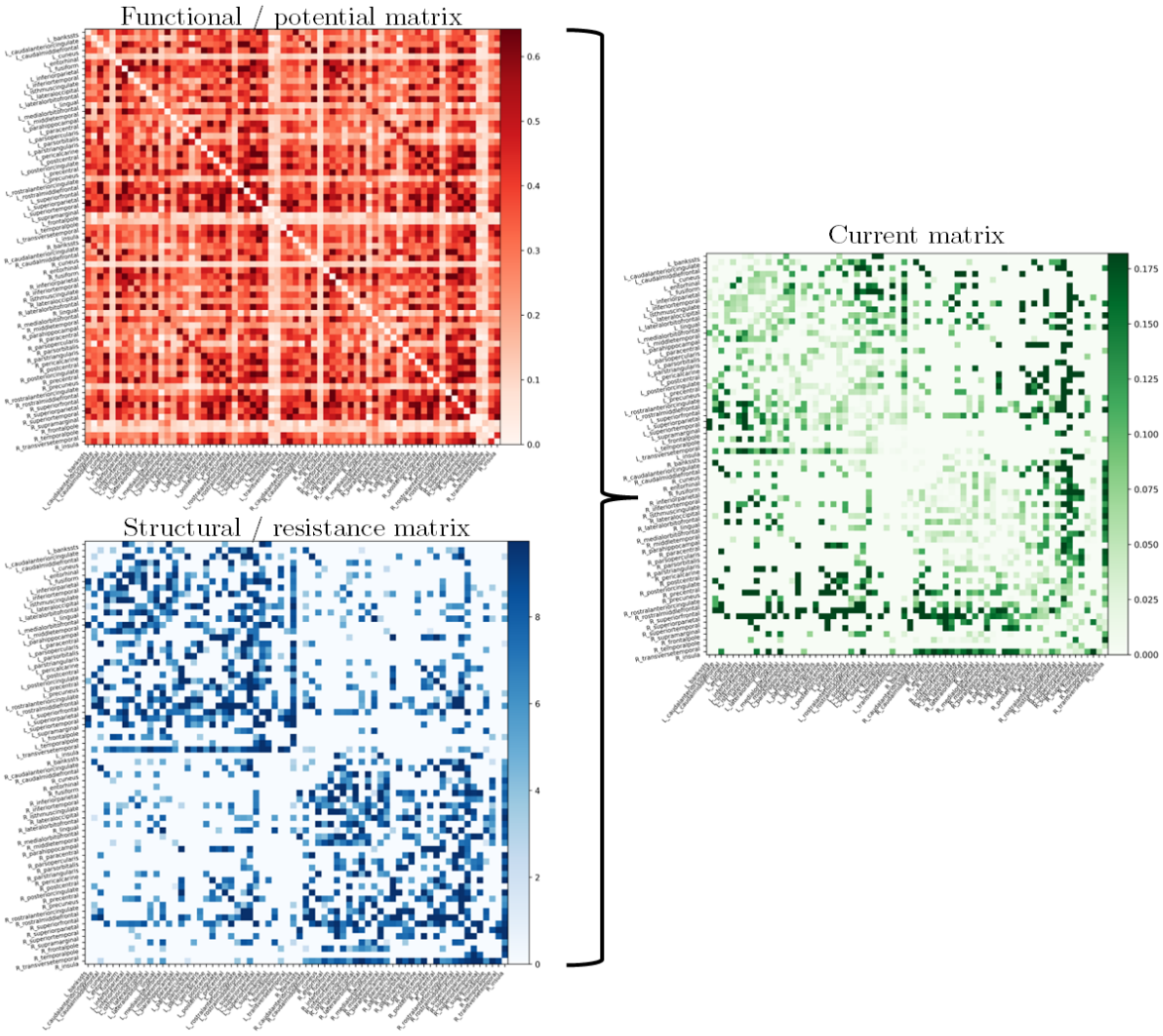

Figure 6: Group-level connectome analysis of 207 subjects from the Human Connectome Project. Functional connectivity (red) and structural connectivity (blue) matrices are shown alongside the resulting current-based connectome (green) derived from the proposed constrained Laplacian coupling. The current-based connectome is notably sparser than either the functional or structural matrices, reflecting that functional relationships are preferentially supported by a subset of anatomically efficient pathways rather than uniformly distributed across all available connections. This sparsity indicates convergence of functional interactions along shared structural routes, yielding a pathway-resolved representation that highlights structurally plausible substrates of functional coupling while suppressing weak or redundant connections.

et al., 2020). The proposed method retains this theoretical basis but introduces an edge-centric perspective, explicitly identifying which structural connections mediate functional relationships. This shift from node-level summaries to pathway-specific in-

sights represents a conceptual advance, enabling tractography filtering and connectivity analyses that are both mathematically consistent and anatomically interpretable.

The framework offers practical benefits. By modeling functional correlations as voltage sources and structural connections as conductances, the resulting current-based connectivity matrix provides actionable information for tractography filtering. The phantom simulation (Figure 5) confirmed that incorporating functional constraints eliminates false-positive streamlines and accurately reconstructs indirect pathways. This information could be used in robust tractography filtering (Sairanen et al., 2021) to utilize multimodal information.

The ability to compute streamline-wise currents (Figure 3) opens new opportunities for along-tract analyses (Colby et al., 2012) and tractometry (Chamberland et al., 2021). Identifying which white matter pathways carry functional information could provide insights into disorders that disrupt connectivity, such as aphasia, where structural changes vary across individuals (Sihvonen et al., 2024). This could support personalized rehabilitation strategies by pinpointing which functional routes are impaired or restored.

Importantly, the proposed framework produces an adjacency-like matrix, making it compatible with existing network analysis tools, including GNNs (Sporns, 2013). Similarly, tractography visualization platforms can readily display streamline-wise currents, as demonstrated in Figure 3. The open-source implementation provided with this study integrates seamlessly with these tools, facilitating adoption within the computational neuroscience community.

In the future, the framework could be extended into dynamic formulations by introducing time-dependent voltage sources and conductance changes, transforming the system in eq. 11 to complete MNA (Wedepohl and Jackson, 2002). This would align with dynamic causal modeling (Friston, 2011) and large-scale dynamic brain models (Breakspear, 2017; Deco, 2015), enabling simulation of transient neural activity and event-driven responses.

In summary, this work bridges spectral graph theory and circuit analysis to create a novel, interpretable representation of structure-function coupling. By preserving Laplacian-based principles while extending them to edge-level modeling, the proposed method provides both theoretical rigor and practical utility. Its interpretability offers unique advantages for tractography filtering and clinical applications. Future studies should explore dynamic extensions and validate the approach in patient populations to fully realize its potential.

References

Abdelnour, F., Dayan, M., Devinsky, O., Thesen, T., and Raj, A. (2018). Functional brain connectivity is predictable from anatomic network's laplacian eigen-structure. *NeuroImage*, 172:728–739.

Abdelnour, F., Voss, H. U., and Raj, A. (2014). Network diffusion accurately models the relationship between structural and functional brain connectivity networks. *Neuroimage*, 90:335–347.

Atasoy, S., Donnelly, I., and Pearson, J. (2016). Human brain networks function in connectome-specific harmonic waves. *Nature communications*, 7(1):10340.

Breakspear, M. (2017). Dynamic models of large-scale brain activity. *Nature neuroscience*, 20(3):340–352.

Breakspear, M., Jirsa, V., and Deco, G. (2010). Computational models of the brain: from structure to function.

Chamberland, M., Genc, S., Tax, C. M., Shastin, D., Koller, K., Raven, E. P., Cunningham, A., Doherty, J., van den Bree, M. B., Parker, G. D., et al. (2021). Detecting microstructural deviations in individuals with deep diffusion mri tractometry. *Nature computational science*, 1(9):598–606.

Chen, P., Yang, H., Zheng, X., Jia, H., Hao, J., Xu, X., Li, C., He, X., Chen, R., Okubo, T. S., et al. (2024). Group-common and individual-specific effects of structure–function coupling in human brain networks with graph neural networks. *Imaging Neuroscience*, 2:1–21.

Chung, F. R. (1997). *Spectral graph theory*, volume 92. American Mathematical Soc.

Colby, J. B., Soderberg, L., Lebel, C., Dinov, I. D., Thompson, P. M., and Sowell, E. R. (2012). Along-tract statistics allow for enhanced tractography analysis. *Neuroimage*, 59(4):3227–3242.

Deco, G. (2015). The dynamics of resting fluctuations in the brain. *BMC Neuroscience*, 16(Suppl 1):A2.

Deslauriers-Gauthier, S., Zucchelli, M., Frigo, M., and Deriche, R. (2020). A unified framework for multimodal structure–function mapping based on eigenmodes. *Medical Image Analysis*, 66:101799.

Dhollander, T., Raffelt, D., and Connelly, A. (2016). Unsupervised 3-tissue response function estimation from single-shell or multi-shell diffusion mr data without a co-registered t1 image. In *ISMRM workshop on breaking the barriers of diffusion MRI*, volume 5. Lisbon.

Fillard, P., Descoteaux, M., Goh, A., Gouttard, S., Jeurissen, B., Malcolm, J., Ramirez-Manzanares, A., Reisert, M., Sakaie, K., Tensaouti, F., et al. (2011). Quantitative evaluation of 10 tractography algorithms on a realistic diffusion mr phantom. *Neuroimage*, 56(1):220–234.

Friston, K. J. (2011). Functional and effective connectivity: a review. *Brain*, 1(1):13–36. MAG ID: 2061564920.

Greaves, M. D., Novelli, L., Mansour L., S., Zalesky, A., and Razi, A. (2025). Structurally informed models of directed brain connectivity. *Nature Reviews Neuroscience*, 26(1):23–41. Publisher: Nature Publishing Group.

Ho, C.-W., Ruehli, A., and Brennan, P. (1975). The modified nodal approach to network analysis. *IEEE Transactions on Circuits and Systems*, 22(6):504–509. Conference Name: IEEE Transactions on Circuits and Systems.

Honey, C. J., Sporns, O., Cammoun, L., Gigandet, X., Thiran, J.-P., Meuli, R., and Hagmann, P. (2009). Predicting human resting-state functional connectivity from structural connectivity. *Proceedings of the National Academy of Sciences*, 106(6):2035–2040.

Hong, Y., Cornea, E., Girault, J. B., Bagonis, M., Foster, M., Kim, S. H., Prieto, J. C., Chen, H., Gao, W., Styner, M. A., et al. (2023). Structural and functional connectome relationships in early childhood. *Developmental Cognitive Neuroscience*, 64:101314.

Huang, H. and Ding, M. (2016). Linking Functional Connectivity and Structural Connectivity Quantitatively: A Comparison of Methods. *Brain*, 6(2):99–108. MAG ID: 2229937548.

Larivière, S., Paquola, C., Park, B.-y., Royer, J., Wang, Y., Benkarim, O., Vos de Wael, R., Valk, S. L., Thomopoulos, S. I., Kirschner, M., Lewis, L. B., Evans, A. C., Sisodiya, S. M., McDonald, C. R., Thompson, P. M., and Bernhardt, B. C. (2021). The ENIGMA Toolbox: multiscale neural contextualization of multisite neuroimaging datasets. *Nature Methods*, 18(7):698–700. Number: 7 Publisher: Nature Publishing Group.

Larivière, S., Rodríguez-Cruces, R., Royer, J., Caligiuri, M. E., Gambardella, A., Concha, L., Keller, S. S., Cendes, F., Yasuda, C., Bonilha, L., Gleichgerrcht, E., Focke, N. K., Domin, M., von Podewills, F., Langner, S., Rummel, C., Wiest, R., Martin, P., Kotikalapudi, R., O'Brien, T. J., Sinclair, B., Vivash, L., Desmond, P. M., Alhusaini, S., Doherty, C. P., Cavalleri, G. L., Delanty, N., Kälviäinen, R., Jackson, G. D., Kowalczyk, M., Mascalchi, M., Semmelroch, M., Thomas, R. H., Soltanian-Zadeh, H., Davoodi-Bojd, E., Zhang, J., Lenge, M., Guerrini, R., Bartolini, E., Hamandi, K., Foley, S., Weber, B., Depondt, C., Absil, J., Carr, S. J. A., Abela, E., Richardson, M. P., Devinsky, O., Severino, M., Striano, P., Tortora, D., Hatton, S. N., Vos, S. B., Duncan, J. S., Whelan, C. D., Thompson, P. M., Sisodiya, S. M., Bernasconi, A., Labate, A., McDonald, C. R., Bernasconi, N., and Bernhardt, B. C. (2020). Network-based atrophy modeling in the common epilepsies: A worldwide ENIGMA study. *Science Advances*, 6(47):eabc6457. Publisher: American Association for the Advancement of Science.

Liu, Z.-Q., Vazquez-Rodriguez, B., Spreng, R. N., Bernhardt, B. C., Betzel, R. F., and Misic, B. (2022). Time-resolved structure-function coupling in brain networks.

Communications biology, 5(1):532.

Neudorf, J., Kress, S., and Borowsky, R. (2022). Structure can predict function in the human brain: a graph neural network deep learning model of functional connectivity and centrality based on structural connectivity. *Brain Structure and Function*, 227(1):331–343.

Poupon, C., Laribiere, L., Tournier, G., Bernard, J., Fournier, D., Fillard, P., Descoteaux, M., and Mangin, J.-F. (2010). A diffusion hardware phantom looking like a coronal brain slice. In *Proceedings of the international society for magnetic resonance in medicine*, volume 18, page 581.

Poupon, C., Rieul, B., Kezele, I., Perrin, M., Poupon, F., and Mangin, J.-F. (2008). New diffusion phantoms dedicated to the study and validation of high-angular-resolution diffusion imaging (hardi) models. *Magnetic Resonance in Medicine: An Official Journal of the International Society for Magnetic Resonance in Medicine*, 60(6):1276–1283.

Raichle, M. E., MacLeod, A. M., Snyder, A. Z., Powers, W. J., Gusnard, D. A., and Shulman, G. L. (2001). A default mode of brain function. *Proceedings of the national academy of sciences*, 98(2):676–682.

Sairanen, V., Ocampo-Pineda, M., Granziera, C., Schiavi, S., and Daducci, A. (2021). Incorporating outlier information into diffusion MR tractogram filtering for robust structural brain connectivity and microstructural analyses. Technical report. Company: Cold Spring Harbor Laboratory Distributor: Cold Spring Harbor Laboratory Label: Cold Spring Harbor Laboratory Section: New Results Type: article.

Shuman, D. I., Narang, S. K., Frossard, P., Ortega, A., and Vandergheynst, P. (2013). The emerging field of signal processing on graphs: Extending high-dimensional data analysis to networks and other irregular domains. *IEEE signal processing magazine*, 30(3):83–98.

Sihvonen, A. J., Pitkäniemi, A., Siponkoski, S.-T., Kuusela, L., Martínez-Molina, N., Laitinen, S., Särkämö, E.-R., Pekkola, J., Melkas, S., Schlaug, G., et al. (2024). Structural neuroplasticity effects of singing in chronic aphasia. *Eneuro*, 11(5).

Smith, R. E., Tournier, J.-D., Calamante, F., and Connelly, A. (2012). Anatomically-constrained tractography: improved diffusion mri streamlines tractography through effective use of anatomical information. *Neuroimage*, 62(3):1924–1938.

Smith, S. M. and Nichols, T. E. (2009). Threshold-free cluster enhancement: addressing problems of smoothing, threshold dependence and localisation in cluster inference. *Neuroimage*, 44(1):83–98.

Sporns, O. (2013). Structure and function of complex brain networks. *Dialogues in Clinical Neuroscience*, 15(3):247–262.

Suárez, L. E., Markello, R. D., Betzel, R. F., and Misic, B. (2020). Linking Structure and Function in Macroscale Brain Networks. *Trends in Cognitive Sciences*, 24(4):302–315.

Tournier, J.-D., Smith, R., Raffelt, D., Tabbara, R., Dhollander, T., Pietsch, M., Christiaens, D., Jeurissen, B., Yeh, C.-H., and Connelly, A. (2019). Mrtrix3: A fast, flexible and open software framework for medical image processing and visualisation. *Neuroimage*, 202:116137.

Van Essen, D. C., Ugurbil, K., Auerbach, E. J., Behrens, T. E., Bucholz, R. D., R. Bucholz, Chang, A., Chen, L., Maurizio Corbetta, Corbetta, M., Della Penna, S., Curtiss, S. W., Della Penna, S., Feinberg, D. A., Glasser, M. F., Heath, A. C., Harel, N., Heath, A. C., Larson-Prior, L. J., Marcus, D. S., Michalareas, G., Moeller, S., Oostenveld, R., Petersen, S., Petersen, S. E., Prior, F. W., Schlaggar, B. L., Smith, S. M., Snyder, A. Z., Xu, J., and Yacoub, E. (2012). The Human Connectome Project: A data acquisition perspective. *NeuroImage*, 62(4):2222–2231. MAG ID: 2020519533.

Wedepohl, L. M. and Jackson, L. (2002). Modified nodal analysis: an essential addition to electrical circuit theory and analysis. *Engineering Science & Education Journal*, 11(3):84–92. Publisher: IET Digital Library.

Yang, H., Winter, S., Zhang, Z., and Dunson, D. (2022). Interpretable ai for relating brain structural and functional connectomes. *arXiv preprint arXiv:2210.05672*.

Zalesky, A., Sarwar, T., Tian, Y., Liu, Y., Yeo, B. T., and Ramamohanarao, K. (2024). Predicting an individual's functional connectivity from their structural connectome: Evaluation of evidence, recommendations, and future prospects. *Network Neuroscience*, 8(4):1291–1309.

6 Acknowledgements

V.S. was supported by the Orion Research Foundation sr and Instrumentarium Science Foundation sr. The authors wish to thank the Finnish Computing Competence Infrastructure (FCCI) for supporting this project with computational and data storage resources. Open access funded by Helsinki University Library.